ISSN 1063-7842, Technical Physics, 2016, Vol. 61, No. 2, pp. 299–301. © Pleiades Publishing, Ltd., 2016.
Original Russian Text © K. Kusaiynov, N.K. Tanasheva, L.L. Min'kov, B.R. Nusupbekov, Yu.O. Stepanova, A.V. Rozhkova, 2016, published in Zhurnal Tekhnicheskoi Fiziki, 2016, Vol. 61, No. 2, pp. 143–145.

SHORT COMMUNICATIONS

Numerical Simulation of a Flow Past a Triangular Sail-Type Blade of a Wind Generator Using the ANSYS FLUENT Software Package

K. Kusaiynov[a], N. K. Tanasheva*[a], L. L. Min'kov[b], B. R. Nusupbekov[a], Yu. O. Stepanova[a], and A. V. Rozhkova[a]

[a] *Buketov State University, Universitetskaya ul. 28, Karaganda, 100028 Kazakhstan*
[b] *National Research Tomsk State University, pr. Lenina 36, Tomsk, 634050 Russia*
**e-mail: Nazgulya_tans@mail.ru*

Received May 25, 2015

Abstract—An air flow past a single triangular sail-type blade of a wind turbine is analyzed by numerical simulation for low velocities of the incoming flow. The results of numerical simulation indicate a monotonic increase in the drag force and the lift force as functions of the incoming flow; empirical dependences of these quantities are obtained.

DOI: 10.1134/S1063784216020158

One of the priority trends in the development of electric power engineering aimed at the solution of environmental problems in Kazakhstan at present is the employment of renewable natural resources and the implementation of programs for energy and resource saving [1]. Since the Kazakhstan territory mainly consists of regions with low annual average values of wind velocities, commercial wind-powered engines of low and moderate power have not been developed, and the application of available wind generator is noneconomic. In this connection, the designing and construction of wind-powered units intended for operation in low-velocity wind flows are topical for Kazakhstan and are in line with priority trends in the development of science in the republic [2–4].

Sail-type windmills possess the unique property to effectively operate at low wind velocities as well as at high velocities due to dynamically variable shape of the working surface under the action of the wind flow [5, 6].

The research for determining the aerodynamic characteristics of a blade of a wind turbine with a dynamically variable shape of the surface was carried out in laboratory conditions. All experimental tests for this purpose were performed in a T–1–M wind tunnel. The main characteristics of the working part of the wind tunnel are as follows: diameter 50 cm, length 80 cm, turbulence intensity 3%, and flow velocity 1–25 m/s. The parameters of a triangular sail-type blade are: right isosceles triangle with legs of 37 cm and a hypotenuse of 52 cm prepared from sail cloth of density $p = 1200$ kg/m^3.

Here, we consider numerical simulation of the air flow with velocity from 2 to 14 m/s past a triangular sail-type blade (Fig. 1) arranged at an angle of attack of 0° in the working chamber of the wind tunnel for a preset sail depth equal to half the base of the triangle (18.5 cm).

The system of equations describing the gas flow has the form [7]

$$\frac{\partial \mathbf{V}}{\partial t} + (\mathbf{V}\nabla)\mathbf{V} = \mathbf{F} - \frac{1}{\rho}\nabla p + \nu\nabla^2\mathbf{V}, \quad (1)$$

$$\mathrm{div}\mathbf{V} = 0. \quad (2)$$

The boundary conditions at the wall are the sticking and no-flow conditions:

$$\mathbf{V} = 0, \quad (3)$$

$$\frac{\partial k}{\partial n} = 0, \quad \varepsilon_P = \frac{C_\mu^{3/4} k_P^{3/2}}{\kappa y_P}, \quad (4)$$

where $k = 0.4187$ is the Karman constant and P corresponds to the center of near-wall cell of the difference grid.

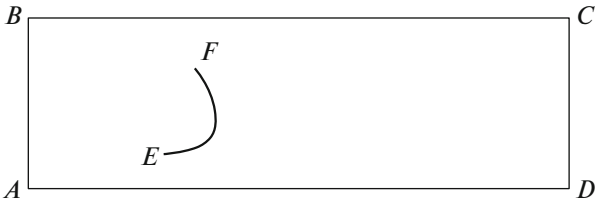

Fig. 1. Numerical integration domain.

Table 1. Dependence of the drag on the wind velocity for 2D and 3D measurements

Velocity, m/s	Drag force	
	2D-measurement	3D-measurement
2	0.11689019	0.11275012
4	0.46832793	0.43586214
5	0.7320603	0.70952331
6	1.0544758	1.0478234

The boundary conditions at the input are

$$U = U_{\text{in}}, \quad V = 0. \tag{5}$$

The turbulent parameters of the flow are determined by specifying turbulent pulsation intensity I and hydraulic diameter D_{hyd}:

$$k = \frac{3}{2}(IV_{\text{inlet}})^2, \quad \varepsilon = C_\mu^{3/4}\frac{k^{3/2}}{l}, \quad l = 0.07D_{\text{hyd}}I = 3\%. \tag{6}$$

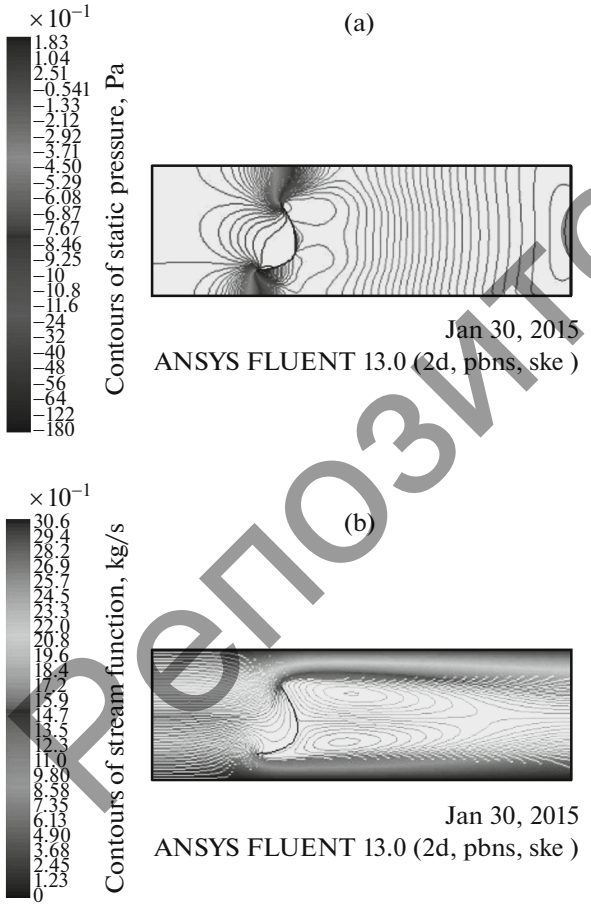

Fig. 2. Distribution fields of (a) pressure and (b) flow lines in the symmetry plane for angle of attack $\alpha = 0°$ and for a velocity of the incoming flow of 5 m/s.

Table 2. Comparison of the drag for different finite-difference meshes

Velocity, m/s	Drag force		
	Mesh C_1	Mesh C_2	Mesh C_3
2	0.12197591	0.11689019	0.11694198
4	0.48873618	0.46832793	0.4683286
5	0.76396827	0.7320603	0.73198883
6	1.1004501	1.0544758	1.0543102

The boundary conditions at the output are

$$\frac{\partial\varphi}{\partial x} = 0. \tag{7}$$

For the k–ε model, we used the standard recommended set of empirical constants, which is usually assumed on default in computing packages:

$$C_\mu = 0.09, \quad C_{\varepsilon 1} = 1.44, \quad C_{\varepsilon 2} = 1.92, \quad \sigma_k = 1.0, \quad \sigma_\varepsilon = 1.3. \tag{8}$$

The size of the computational domain was chosen in accordance with the sizes of the wind tunnel. It was a rectangular region with a model placed into it (Fig. 1). The finite-difference mesh was constructed using the Gambit 2.3.16 code.

For choosing the measuring system, computations were performed in the 2D and 3D formulations of the problem. Table 1 contains the results of calculation of the drag force for 2D and 3D measurements.

It can be seen from Table 1 that the drags in the 2D and 3D formulations differ insignificantly. Therefore, we can use the 2D formulation to simplify computations.

To determine the effect of the computation mesh (number of cells) on the result of determining the drag of the triangular blade with the help of the model used here, calculations were made for three computational meshes with (*1*) 20000, (*2*) 40000, and (*3*) 160000 points.

Table 2 shows the drag forces obtained for low wind velocities from 2 to 6 m/s. The values of C_1, C_2, and C_3 correspond to the drags obtained on meshes with 20000, 40000, and 160000 points, respectively.

It can be seen from Table 2 that the discrepancy in the values of drag for meshes with 40000 and 160000 points is insignificant, while the difference in the value of drag obtained on the mesh with 20000 points is noticeable. Therefore, it is expedient to use the mesh with 40000 points for calculations.

Numerical simulation was carried out using the ANSYS Fluent program package on the basis of solution of 2D equations (1) and (2) with boundary conditions (3)–(8) with the help of the Patankar method [8], implicit algorithm of the second order of accuracy

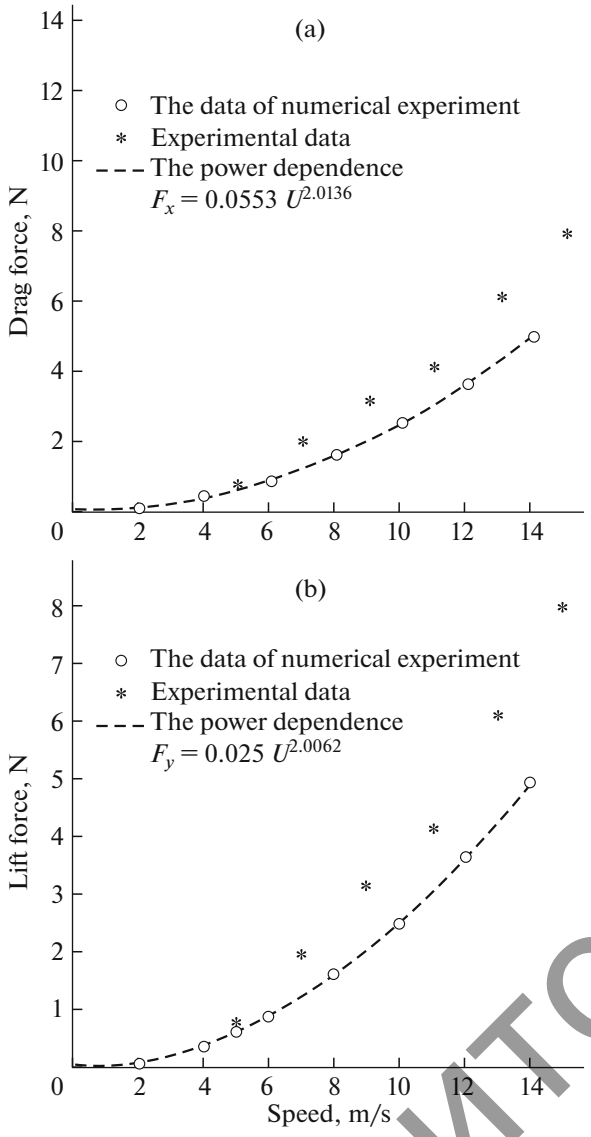

Fig. 3. Dependences of (a) drag force and (b) lift force on the velocity of the incoming flow.

over the space for convective terms of the equations, and the k–ε two-parametric turbulence model.

Figure 2 shows the pressure distribution fields and flow lines in the symmetry plane for angle of attack $\alpha = 0°$ and for an incoming flow velocity of 5 m/s.

It can be seen that a reverse–circulation flow is formed behind the body, and high-pressure regions appear on the blade surface.

Figure 3 shows the dependence of the drag and lift forces on the velocity of the incoming flow. Circles correspond to the results of numerical experiment and asterisks are experimental data; the dashed curve approximates the results.

Figure 3a shows the results of numerical experiment approximated by the power dependence $F_x = 0.0553U^{2.0136}$.

It can be seen that the results of calculation are in good agreement with experimental data. The drag force increases with the velocity of the incoming flow.

Figure 3b shows the results of numerical experiment on determining the lift force, which are approximated by the power dependence $F_y = 0.025U^{2.0062}$.

The discrepancy between the experimental data and the results of numerical simulation is of about 3–4%. This can be explained by the experimental error of 3%.

On the basis of numerical simulation, universal dependences of the aerodynamic parameters on the geometry of the blade profile have been established for various velocities of the wind flow. The results of simulation of the flow past a triangular sail-type blade have been obtained. Comparison of the results of numerical calculations with experimental data demonstrates satisfactory agreement.

The regularities in the variation of the aerodynamic parameters established in this study can be useful for understanding the complex aerodynamic pattern of the turbulent air flow past bodies with various profiles. The universal dependences obtained for the driving force and drag can be used in designing sail-type wind turbines.

REFERENCES

1. A. V. Bolotov, S. E. Sokolov, and S. A. Bolotov, Vestnik Almatinsk. Inst. Energ. Svyazi, No. 3(6), 11 (2009).
2. K. Kussaiynov, N. K. Tanasheva, M. M. Turgunov, and K. M. Shaimerdenova, Mod. Appl. Sci. **9**, 218 (2015).
3. K. Kussaiynov, N. K. Tanasheva, M. M. Turgunov, and A. R. Alibekova, Tech. Phys. **60**, 656 (2015).
4. K. Kussaiynov, S. E. Sakipova, N. K. Tansykbaeva, and A. Kussaiynova, *Proceedings of the 7th International Symposium on Turbulence, Heat and Mass Transfer, Palermo, Italy, 2012,* Vol. 7, p. 577.
5. K. Kusaiynov, Zh. T. Kambarova, N. K. Tanasheva, K. M. Shaimerdenova, and A. R. Alibekova, Inzh.-Fiz. Zh. **88** (2), 23 (2015).
6. D. Yu. Zhilenko and O. E. Krivonosova, Tech. Phys. Lett. **41**, 5 (2015).
7. S. A. Isaev, P. A. Baranov, A. G. Sudakov, and A. M. Ermakov, Tech. Phys. Lett. **41**, 76 (2015).
8. S. Patankar, *Numeral Heat Transfer and Fluid Flow* (McGraw-Hill, New York, 1980).

Translated by N. Wadhwa